chemosensors

Article

Adsorption Properties of ZSM-5 Molecular Sieve for Perfluoroisobutyronitrile Mixtures and Its Fluorocarbon Decomposition Products

Wei Liu [1], Xinjie Qiu [1], Xiaoxing Zhang [2], Shuangshuang Tian [2,*], Zian Yuan [2] and Weihao Liu [2]

[1] Electric Power Research Institute, Anhui Electric Power Co., Ltd., Hefei 230601, China; sgccliu@163.com (W.L.); qiuxj2141@ah.sgcc.com.cn (X.Q.)
[2] Hubei Engineering Research Center for Safety Monitoring of New Energy and Power Grid Equipment, Hubei University of Technology, Wuhan 430068, China; zhangxx@hbut.edu.cn (X.Z.); 102000197@hbut.edu.cn (Z.Y.); 102110377@hbut.edu.cn (W.L.)
* Correspondence: tianss@hbut.edu.cn

Abstract: Perfluoroisobutyronitrile (C_4F_7N), an environment-friendly insulating gas, has excellent insulating properties and has the potential to be used in gas-insulated equipment when mixed with CO_2. Selecting suitable adsorption materials to adsorb the decomposition products of the C_4F_7N mixture can ensure the safe and stable operation of the gas-insulated equipment and the personal safety of the operators in the electric power industry. The adsorption characteristics of the ZSM-5 molecular sieve on C_4F_7N and its five fluorocarbon decomposition products were investigated by adsorption experiments. The results show that the ZSM-5 molecular sieve has a certain adsorption effect on six fluorocarbon gases; the adsorption performance of C_3F_6 and C_3F_8 are the best, with an adsorption efficiency over 85%, while the concentration of CO_2 and C_4F_7N is affected by the ZSM-5 molecular sieve. At the same time, the paper based on the Metropolis Monte Carlo simulation of Materials Studio software found that the ZSM-5 molecular sieve has the strongest adsorption effect on C_4F_7N molecules and the weakest adsorption effect on CO_2 molecules. The stronger the polarity of the gas molecule, the more obvious the adsorption effect of molecular sieve structure on it. As a result, the ZSM-5 molecular sieve could be used in tail gas purification of insulated equipment, as well as to provide solutions for the development and production of protective equipment.

Keywords: C_4F_7N/CO_2 mixtures; fluorocarbon decomposition products; ZSM-5 molecular sieve; gas adsorption; molecular dynamics simulation

Citation: Liu, W.; Qiu, X.; Zhang, X.; Tian, S.; Yuan, Z.; Liu, W. Adsorption Properties of ZSM-5 Molecular Sieve for Perfluoroisobutyronitrile Mixtures and Its Fluorocarbon Decomposition Products. *Chemosensors* **2022**, *10*, 121. https://doi.org/10.3390/chemosensors10040121

Academic Editor: Andrea Ponzoni

Received: 15 February 2022
Accepted: 18 March 2022
Published: 24 March 2022

1. Introduction

SF_6 is a stable gas with excellent insulation and arc extinguishing performance, which is widely used in various gas insulation equipment However, the global warming potential (GWP) value of SF_6 is high, about 23,500 times that of CO_2. In the "Kyoto Protocol" promulgated in 1997, it was clearly stated that SF_6 is a greenhouse gas [1–4]. With the increasing global greenhouse effect on the environment, the control of greenhouse gas emissions has become the primary task of protecting the global environment. Some countries and regions have introduced policies and regulations to limit the usage and emissions of SF_6. Particularly, China has pledged to reduce SF_6 emissions to 55~60% of 2005 levels by 2019 [5]. It is one of the research hotspots to find a new type of environment-friendly insulating medium that can replace SF_6 in the electric power industry. 3M, in conjunction with General Electric, introduced the "g3", an environmentally friendly insulating gas, which is mainly 4~10% perfluoroisobutyronitrile (C_4F_7N) and CO_2. The insulation performance of C_4F_7N is about twice that of SF_6, and the GWP of C_4F_7N is only 2090. Although the liquefaction temperature is high (−4.7 °C), it has potential application in engineering when mixed with a buffer gas (CO_2, N_2) [6,7].

At present, a new type of environment-friendly insulating gas has been put into trial operation in a variety of gas-insulated equipment, and good progress has been made in the development of insulating equipment using C_4F_7N/CO_2 as the medium. However, when the gas-insulated equipment is operated for a long time, the insulating medium will decompose due to discharge and overheating [8–10]. Simka et al. have found that C_4F_7N mixtures can produce C_2F_3N and C_2N_2 toxic gases in partial discharge [11]. Radisavljevic et al. analyzed the gas after C_4F_7N arc discharge and found cyanides such as CF_3CN and C_2F_5CN [12]. Li et al. studied the decomposition products of C_4F_7N/CO_2 mixtures under different operating conditions; the results show that CO, CF_4, C_2F_6, C_2F_4, CF_3H, C_3F_8, C_3F_7H, C_2F_3N, C_3F_6, C_4F_6, C_4F_{10}, C_3F_5N, C_2N_2, C_4F_8, and HCN [13] are the possible decomposition products under different fault conditions. To ensure that some of the decomposition products will not interfere with the insulation performance of the insulating medium and ensure the long-term stable operation of the equipment, the equipment will be equipped with porous absorbent materials to adsorb the decomposition products.

Many studies have been carried out on the adsorption of decomposition products of C_4F_7N mixtures, and it is considered that molecular sieve and activated alumina materials have the potential to be used in gas-insulated equipment [14,15]. F. Meyer et al. studied the adsorption properties of 3A, 4A, and 5A molecular sieves for decomposition products CF_3CN, C_2F_5CN, and COF_2 [16]. Han et al. compared and analyzed the adsorption characteristics of γ-Al_2O_3 and molecular sieves (3A, 4A, and 5A) on C_4F_7N/CO_2 mixtures and their decomposition products. The experimental results show that γ-Al_2O_3 and molecular sieves have weak adsorption capacity for buffer gas CO_2 and decomposition products of CO and perfluorocarbon gases, but they can selectively adsorb nitrile gases, and the other four adsorbents can effectively adsorb the CNCN. γ-Al_2O_3 and 5A molecular sieve can effectively adsorb the CF_3CN [17]. The team of Hua simulated the adsorption performance of the C_4F_7N/CO_2 mixtures and its 13 decomposition products in Na-4A molecular sieve through molecular dynamics simulation methods. They calculated saturated adsorption capacity, adsorption isotherm, adsorption free energy, and other thermodynamic parameters and found that the Na-4A molecular sieve has weak adsorption capacity for perfluoroalkanes and olefins, and can efficiently adsorb various highly toxic decomposition products [18]. Based on the existing research, the adsorption of carbon and fluorine decomposition products of the C_4F_7N/CO_2 mixtures is not clear. Some fluorocarbon gases, hexafluoroethane (C_2F_6) and octafluoropropane (C_3F_8) have high greenhouse effect potential and atmospheric lifetime [19]. Some fluorocarbon gases, fluoroform (CF_3H), Carbon tetrafluoride (CF_4), and hexafluoropropylene (C_3F_6) are toxic which would cause adverse reactions after human inhalation [20–22]. Therefore, it is necessary to select suitable adsorbents to efficiently adsorb and treat the above-mentioned gases. In the selection of adsorbents, the pore diameter of the selected molecular sieve materials is mostly no more than 0.5 nm, and the adsorption effect of these materials on the larger gas molecules is not obvious. In this paper, the ZSM-5 molecular sieve with 0.55 nm pore diameter was selected to investigate the adsorption properties of five fluorocarbon decomposition products (CF_3H, CF_4, C_2F_6, C_3F_6, and C_3F_8) for the C_4F_7N mixtures and the main insulating gases (C_4F_7N and CO_2). Then the adsorption experiment of the standard gases of the above eight gases was carried out, and the concentrations were measured before and after the experiment by gas chromatography-mass spectrometer (GCMS) and Fourier infrared spectrometer (FTIR). Finally, the adsorption properties of ZSM-5 molecular sieve for all gases were evaluated by the reduction of concentration. In addition, the adsorption heat and other parameters are calculated by the method of molecular dynamics simulation in this paper. The results provide a reference for the selection of the adsorption materials in environmentally friendly insulated gas power equipment.

2. ZSM-5 Adsorption Experiment

2.1. Adsorption Experiment Method

Considering the actual concentration of C_4F_7N mixtures and common fluorocarbon gases, the relevant parameters of the adsorbate gas concentration used in this paper are shown in Table 1. The dilution background of each low-concentration standard gas was He, and the concentration error was ±3 ppm. The three adsorbate gases with high concentrations were made up of 99.2% C_4F_7N, 99.999% CO_2, and 99.999% He. The ZSM-5 molecular sieve material was provided by Pioneer Nano Company, and the adsorption experimental device is shown in Figure 1. The detailed experimental procedure is shown in Table 2.

Table 1. The concentration of adsorbate gas in the experiment.

Type of Gas	CF_3H	CF_4	C_2F_6	C_3F_6	C_3F_8	C_4F_7N Standard Gas	CO_2 Standard Gas	Gas Mixtures
concentration	200 ppm	200 ppm	200 ppm	200 ppm	200 ppm	15%C_4F_7N/85%He	15%CO_2/85%He	15%C_4F_7N/85%CO_2

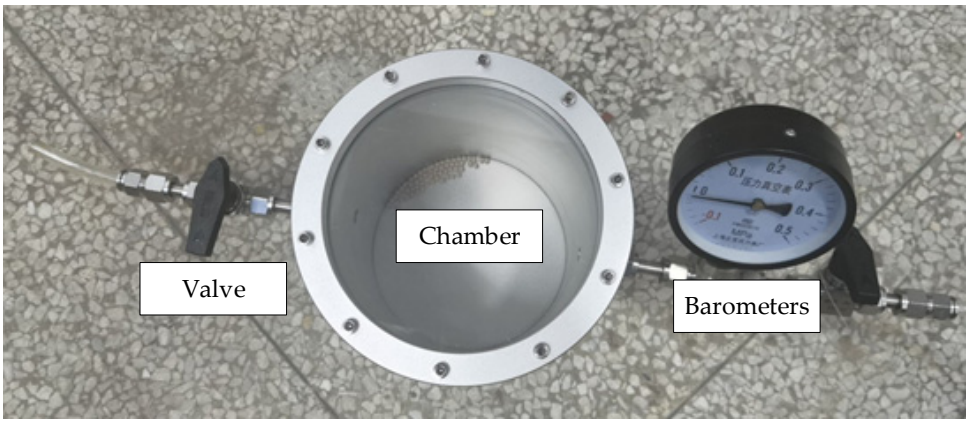

Figure 1. Adsorption experimental device.

Table 2. Experimental procedure.

Step	Operation Content
①	Checking the tightness of the device
②	Loading with 3 g of adsorption material
③	Pumping of the chamber to vacuum
④	Heating activates the adsorbent
⑤	Vacuuming for five minutes to remove the residual impurity gas in the chamber
⑥	Filling the chamber with gas to an absolute pressure of 0.15 MPa, and then letting it stand for 48 h.
⑦	Detecting the concentration of the gas in the chamber after 48 h

2.2. Concentration Detection

For the concentration detection of low-concentration gases (CF_3H, CF_4, C_2F_6, C_3F_6, and C_3F_8), the instrument used was a Shimadzu QP-2020NX gas chromatography-mass spectrometer, equipped with a special capillary column (CP-Sil5CB) for gas qualitative determination detection, using 99.999% He as carrier gas. The column temperature adopted the programmed heating method: 0–9 min maintained at 32 °C unchanged, then the temperature was raised to 120 °C at a constant rate for 3 min after 9 min, and finally

the temperature was kept unchanged to maintain the temperature at 120 °C. The inlet temperature was 200 °C, the split ratio was 50:1, the 200 °C EI ion source was used as the MS ion source, and the sample inlet temperature was 200 °C. After gas sampling, ion scanning was used to quantitatively analyze the characteristic ions of each fluorocarbon gas. The corresponding characteristic ion mass-to-charge ratios (m/z) of the six gases were 69, 69, 119, 131, 69, respectively.

For the detection of high-concentration gases (C_4F_7N and CO_2), the instrument used was a Thermo Scientific Nicolet iS50 infrared spectrometer. The optical path length of the gas cell in the infrared spectrometer was 2.4 m, the volume was 200 mL, and the material of the windows at both ends of the gas cell was potassium bromide. The number of scans was set to 1 and the resolution to 4 before collecting the absorption spectrum signal. A specific absorption peak was selected and the intensity of each gas absorption peak was compared before and after the experiment to quantitatively analyze the change in concentration. For the analysis of C_4F_7N concentration, the characteristic peaks in the range of 2220~2290 cm^{-1} were selected. For CO_2 concentration analysis, characteristic peaks with wavenumbers ranging from 3650 to 3755 cm^{-1} were selected.

2.3. Analysis of Results

Figure 2 shows the concentration changes of six low-concentration fluorocarbon decomposition products before and after the adsorption experiment.

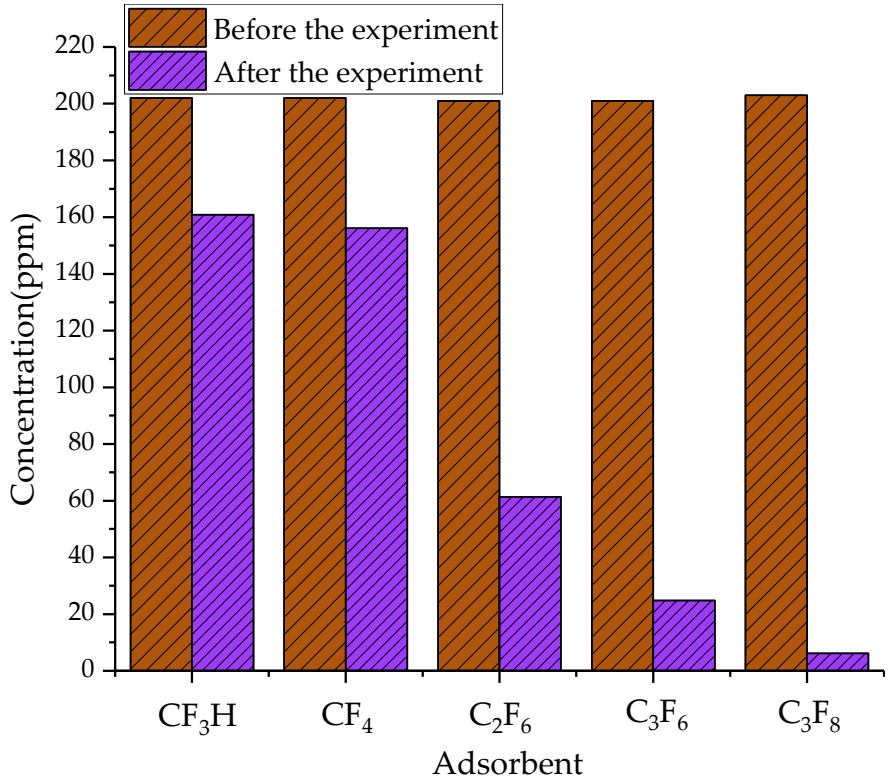

Figure 2. The concentration of fluorocarbon gases before and after the experiment.

It can be seen from the figure that the concentration of each gas decreased after the experiment. The adsorption properties of the ZSM-5 molecular sieve for five kinds of fluorocarbons were different, and the adsorption properties for C_3F_6 and C_3F_8 were the best. The concentrations of the three gases decreased from 200 ppm to 25 ppm, and 6 ppm respectively, and the adsorption efficiency was over 85%. The concentration of C_2F_6 decreased from 200 ppm before the experiment to 61 ppm after the experiment, and the adsorption efficiency was over 65%, but it was weaker than that of C_3F_6 and C_3F_8. The concentration of CF_3H and CF_4 decreased from 200 ppm before the experiment to

161 ppm and 156 ppm after the experiment, and the adsorption efficiency did not exceed 25%. In general, the ZSM-5 molecular sieve adsorbed most of the fluorocarbon gases, although the adsorption performance of some fluorocarbon gases was not outstanding, and the concentration of fluorocarbon decomposition products produced by the equipment due to various failures generally did not exceed the concentration parameters set in this paper. Thus, ZSM-5 molecular sieve could adsorb fluorocarbon decomposition products in electrical insulation equipment.

Figure 3a shows the characteristic peaks corresponding to the 15% C_4F_7N standard gas before and after the experiment. The figure shows that the characteristic peak of C_4F_7N had no obvious change after the experiment, and the two characteristic peak curves coincide. Comparing the absorbance in the 2260~2280 cm^{-1} band, the absorbance of the characteristic peak before the experiment was slightly higher than the absorbance after the experiment, which shows that the ZSM-5 molecular sieve exhibited a partial adsorption capacity for C_4F_7N. Figure 3b shows the characteristic peaks corresponding to the 15% CO_2 standard gas before and after the experiment. The curve of absorbance changes with the number before and after the experiment was roughly the same in this band. When the wave number was constant, the absorbance before the experiment was slightly higher than that after the experiment, so the ZSM-5 molecular sieve also shows partial adsorption capacity to CO_2.

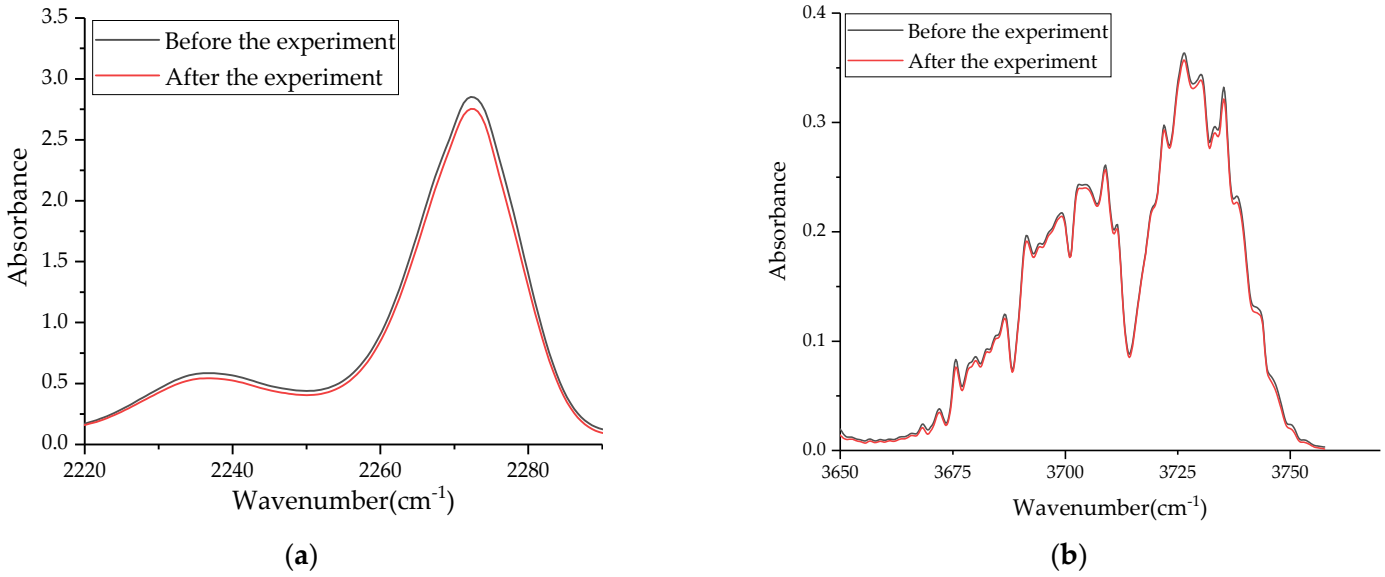

Figure 3. Concentration variation of standard gases of C_4F_7N and CO_2 before and after the experiment. (**a**) 15% C_4F_7N−85% He Infrared spectrometry before and after the experiment; (**b**) 15% CO_2−85% He Infrared spectrometry before and after the experiment.

To calculate the change of main gas concentration before and after the experiment, this paper used Beer-Lambert law to calculate the two concentrations after the experiment through the relevant parameters of the standard gas concentration and the light absorption degree before the experiment [23]. To ensure the accuracy of the calculation results, this paper used two parameters, the peak area of the characteristic peak and the intensity of the absorbance, to estimate the concentration reduction after the experiment. Figure 4 shows the changes of the two parameters of the two gases before and after the experiment.

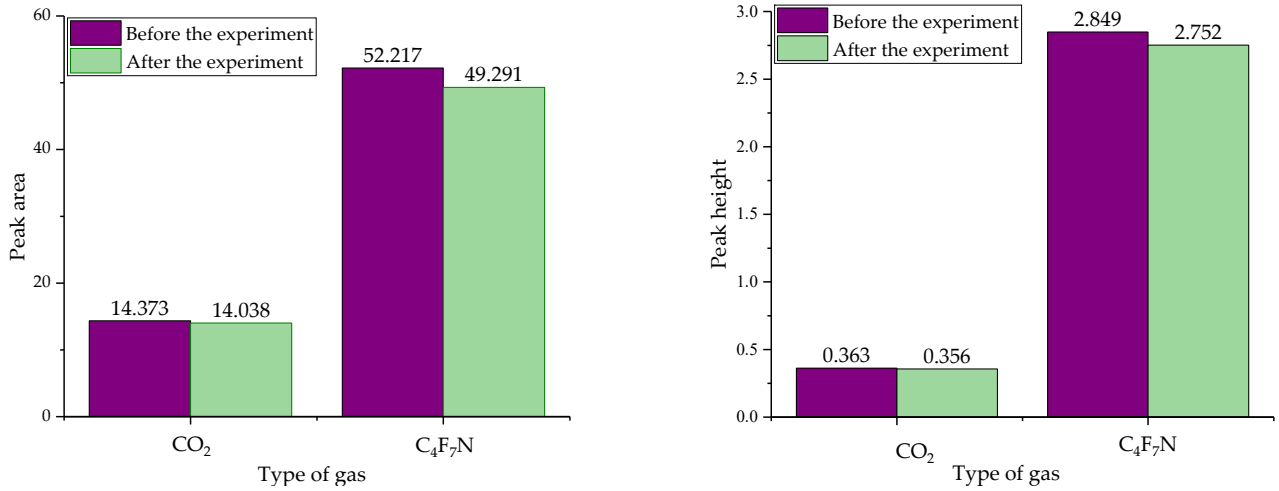

Figure 4. The characteristic peak area and absorbance intensity of C_4F_7N and CO_2 before and after the adsorption experiment. (**a**) Area of characteristic peak; (**b**) Intensity of absorbance.

In the infrared absorption spectrum of C_4F_7N, the curve in the 2260~2290 cm^{-1} band was integrated to calculate the peak area of the characteristic peaks before and after the experiment. The intensity of the absorbance corresponding to the wave velocity of 2272 cm^{-1} was selected to quantitatively analyze the concentration of C_4F_7N before and after the experiment. In the infrared absorption spectrum of CO_2, the curve in the band of 3650~3755 cm^{-1} was integrated, the peak area of the characteristic peak was calculated, and the intensity of the absorbance corresponding to the wave velocity of 3725 cm^{-1} was selected to quantitatively analyze the CO_2 concentration before and after the experiment. Figure 4a shows the corresponding characteristic peak areas of the two gases before and after the experiment, and Figure 3b shows the corresponding absorbance intensities of the two gases before and after the experiment. It can be seen from Figure 4 that the parameters of the two gases after the experiment were lower than before the experiment. To reflect the adsorption efficiency of the ZSM-5 molecular sieve material for the two gases, the adsorption rate was calculated according to the characteristic peak area before and after the experiment and the decrease in absorbance intensity.

Table 3 shows the absorption rate of CO_2 and C_4F_7N in the ZSM-5 molecular sieve calculated with two parameters. Comparing the calculation results of the adsorption rate of the two gases, the adsorption rate calculated by the characteristic peak area was slightly higher than the result calculated by the intensity of the absorbance. From the perspective of the adsorption effect, the error calculated by the two methods can be ignored. According to the calculated adsorption rate of the two gases, the adsorption effect of ZSM-5 molecular sieve on CO_2 and C_4F_7N was not obvious, the average absorption rate of CO_2 was 2.1%, and the average adsorption rate of C_4F_7N was 4.5% [23].

Table 3. Adsorption rates of CO_2 and C_4F_7N standard gases by ZSM-5 molecular sieve.

	Peak Area	**Absorbance Intensity**
adsorption rate of CO_2	2.3%	1.9%
adsorption rate of C_4F_7N	5.6%	3.4%

Figure 5 shows the infrared spectra of C_4F_7N and CO_2 in the gas mixtures before and after the adsorption experiment. The concentration of C_4F_7N and CO_2 in the gas mixtures before and after the experiment is calculated by the characteristic peak area and peak intensity. Table 4 shows the adsorption rates of CO_2 and C_4F_7N in ZSM-5 molecular sieve for different parameters in the gas mixtures. It can be seen from Table 3 that the

concentration of CO_2 after the adsorption experiment is slightly higher than that before the experiment, and the average adsorption rate is −2.05%. The concentration of C_4F_7N is lower than that before the experiment, and the average adsorption rate is 5.9%. It shows that the ZSM-5 molecular sieve in the mixed gas mainly adsorbs C_4F_7N gas, and C_4F_7N inhibits the adsorption of CO_2.

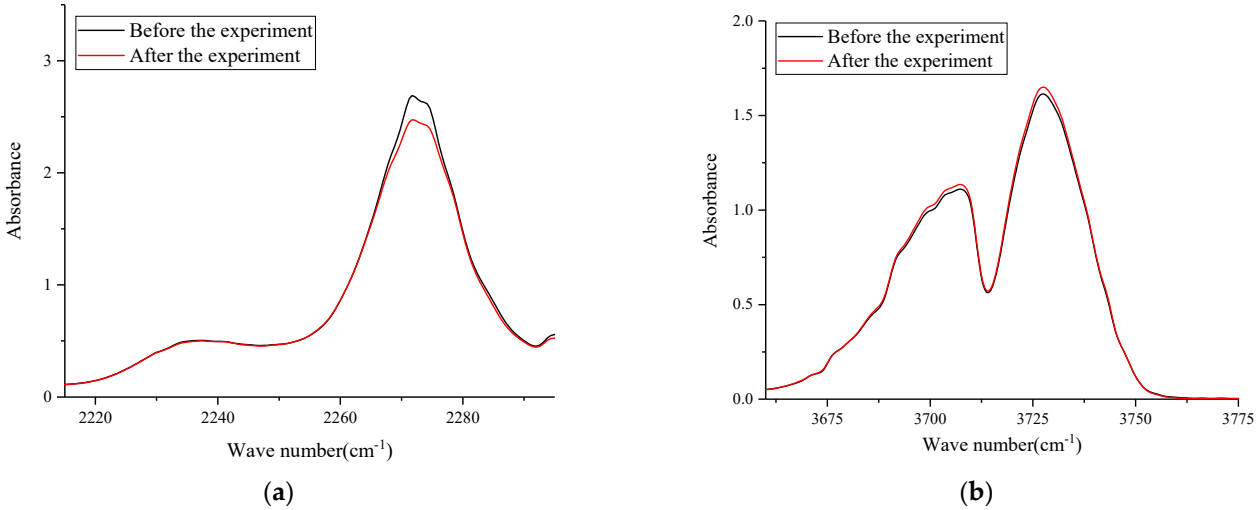

Figure 5. Infrared spectra of 15% C_4F_7N−85% CO_2 gas mixtures before and after the experiment. (**a**) C_4F_7N; (**b**) CO_2.

Table 4. Adsorption rates of CO_2 and C_4F_7N in gas mixtures by ZSM-5 molecular sieve.

	Peak area	Absorbance intensity
adsorption rate of CO_2	−1.8%	−2.3%
adsorption rate of C_4F_7N	3.9%	8.0%

ZSM-5 molecular sieve has good adsorption capacity for most of the fluorocarbon decomposition products of the environmentally friendly insulating medium C_4F_7N/CO_2 mixtures and can achieve complete adsorption for a few fluorocarbon gases. It has the potential to be used in the treatment and purification of exhaust gas from gas-insulated equipment, and it can also provide solutions for the development and production of related protective equipment. However, the ZSM-5 molecular sieve also has a certain adsorption effect on the main insulating medium; specifically, it would affect the concentration of C_4F_7N in the mixtures. If the ZSM-5 molecular sieve can not only adsorb the fluorocarbon decomposition products but also ensure that the insulation performance of the gas is not affected, the proportion of C_4F_7N in the mixture can be increased to 1.04~1.08 times.

3. Adsorption Simulation

3.1. Model Building and Parameter Setting

To clarify the adsorption mechanism and real adsorption capacity of ZSM-5 zeolite porous materials for several fluorocarbon molecules and main insulating gases from the microstructure, the adsorption process was simulated by using the adsorption module in Materials studio simulation software. The initial model was built according to the ZSM-5 molecular sieve in the International Molecular Sieve Association (IZA) database. The simulation was performed using 2 × 2 × 2 cells with cell parameters: a = 4.00 nm, b = 3.98 nm, c = 5.34 nm, $\alpha = \beta = \gamma = 90°$. To be close to the actual experimental molecular sieve structure composition, the Si atoms in the initial model were randomly replaced with Al atoms, and then the Na^+ equilibrium charge was introduced. The optimized structure of NaZSM-5 with a Si/Al ratio of 47 is shown in Figure 6, which consists of vertical straight channels (5.3 × 5.6 Å) and transverse S-shaped channels (5.5 × 5.1 Å).

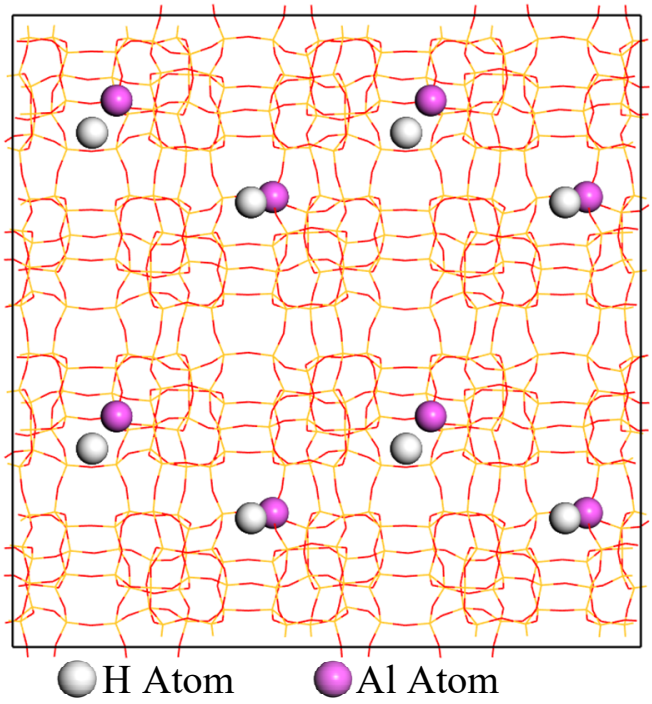

Figure 6. NaZSM-5 molecular sieve model.

According to reference [24], the atomic distribution charges in adsorption are as follows: O(−0.4 e), Si(+0.766 e), Al(+0.575 e), Na (+1 e). The model structures of the five carbon-fluorine decomposition products and two main insulating gas molecules were optimized using the GGA and PBE basis groups in the Dmol3 module. The lowest energy configuration obtained is shown in Figure 7, and the corresponding atomic charge distribution and dynamic diameter are shown in Table 5. The seven gas molecules were introduced into NaZSM-5 separately for kinetic simulations.

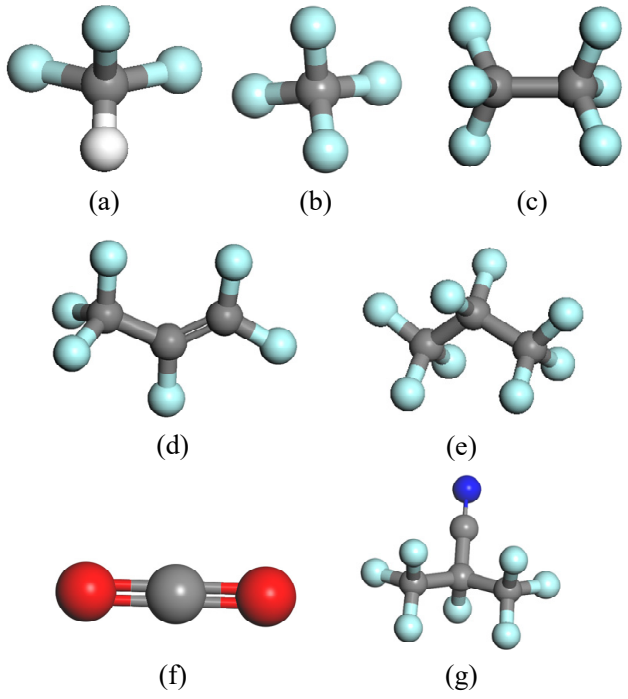

Figure 7. Adsorbent molecular model (**a**) CF_3H; (**b**) CF_4; (**c**) C_2F_6; (**d**) C_3F_6; (**e**) C_3F_8; (**f**) CO_2; (**g**) C_4F_7N.

Table 5. Atomic charge distribution in gas molecules.

Molecule	Charge (e)					Dynamic Diameter (Å)
	C	F	N	H	O	
CF_4	+1.66	−0.41; −0.41; −0.41; −0.41	-	-	-	4.89
C_2F_6	+1.35; +1.35	−0.45; −0.45; −0.45; −0.45; −0.45; −0.45	-	-	-	6.24
C_3F_6	+1.11; −0.23; −1.65	−0.38; −0.40; −0.45; −0.41; −0.48; −0.41	-	-	-	7.25
C_3F_8	+1.37; +1.02; +1.37	−0.50; −0.46; −0.50; −0.46; −0.46; −0.46; −0.46; −0.46	-	-	-	7.44
CF_3H	+0.98	−0.38; −0.38; −0.38	-	+0.16	-	6.21
CO_2	+0.60	-	-	-	−0.30; −0.30	5.15
C_4F_7N	−0.14; +1.64; +1.64;+0.98	−0.43; −0.45; −0.46; −0.47; −0.45; −0.42; −0.46	−0.98	-	-	7.45

The simulation is based on the Metropolis sampling method, and the non-bond interaction is described by the Lennard-Jones potential energy and Coulomb interaction:

$$U(r) = \sum_{i,j}\sum_{i\neq j} 4\varepsilon_{ij}\left[\left(\frac{\sigma_{ij}}{r_{ij}}\right)^{12} - \left(\frac{\sigma_{ij}}{r_{ij}}\right)^{6}\right] + \frac{q_i q_j}{4\pi\varepsilon_0 r_{ij}} \quad (1)$$

In Equation (1), U is the interaction potential energy between two molecules, i and j are different atoms, σ is the position diameter, ϵ is the depth of the potential well, q is the charge parameter set for each atom, and ϵ_0 is the vacuum dielectric constant. Combined with the actual operating environment of the equipment, the pressure was set to 0.15 MPa and the temperature was set to 300 K in the simulation process. The Universal Force Field was selected for simulation. Both the molecular sieve model and the adsorbate gas molecules were regarded as rigid structures. Electrostatic and van der Waals interactions were calculated by Ewald and atom-based methods respectively [24,25]. The 1×10^6 step of the Monte Carlo method process was used to keep the balance, and the 1×10^5 step was used to calculate the heat of adsorption of the gas molecules in the porous structure. The Lennard-Jones parameters of molecular sieve and adsorbent atom based on universal force field are shown in Table 6.

Table 6. Atomic Lennard-Jones parameters in molecular sieves.

Atom	σ/Å	ε/kJ·mol^{-1}
Si	4.27	1.30
Al	4.39	1.30
O	3.40	0.40
Na	3.14	2.10
C	3.89	0.39
N	3.66	0.32
F	3.47	0.30
H	3.19	0.06

3.2. Analysis of Simulation Results

Figure 8 shows the distribution of seven gas molecules in the structure of the NaZSM-5 molecular sieve after the adsorption simulation, and the red dots in the molecular sieve structure indicate the possible locations of gas molecules being adsorbed. From the Figure, the adsorption sites of CF_3H and CF_4 molecules in the carbon-fluorine decomposition product molecules are widely distributed in the molecular sieve structure, with adsorption

sites in both S-type pore channels and straight pore channels. This indicates that CF_3H and CF_4 molecules are small in size and can diffuse freely in the molecular sieve structure, and the skeleton of the molecular sieve does not have a significant inhibitory effect on the two gas molecules. The adsorption sites of C_2F_6, C_3F_6, and C_3F_8 molecules are mainly distributed at the intersection of S-type pore channels and straight pore channels, and a few adsorption sites are in the longitudinal straight pore channels. This shows that the volume of these three gas molecules is larger than the diameter of the S-shaped pore channel, and it is difficult to enter the pore channel and interact with the internal atoms, and the molecular sieve skeleton has a binding effect on the movement of the three gas molecules. From Figure 8f, the adsorption sites of CO_2 molecules are distributed in two different pore channels in the molecular sieve structure. On the one hand, the CO_2 molecules are small in size, and the molecules can move across the pore channels from one pore cage to another when they diffuse; on the other hand, the atoms on the molecular sieve skeleton have an average interaction potential for CO_2 molecules, and there is no significant difference in the adsorption produced by the pore cages and pore channels. The adsorption sites of C_4F_7N molecules in the molecular sieve structure are mainly concentrated at the pore crossings. The range of C_4F_7N adsorption sites is smaller than the range of the three bulkier fluorocarbon gases. This can indicate that C_4F_7N molecules are larger than the molecular sieve pore size, and it is difficult to cross the pores to enter the inside of the molecular sieve structure, so intermolecular forces are generated mainly with the atoms on the pore cage to bind the C_4F_7N molecules.

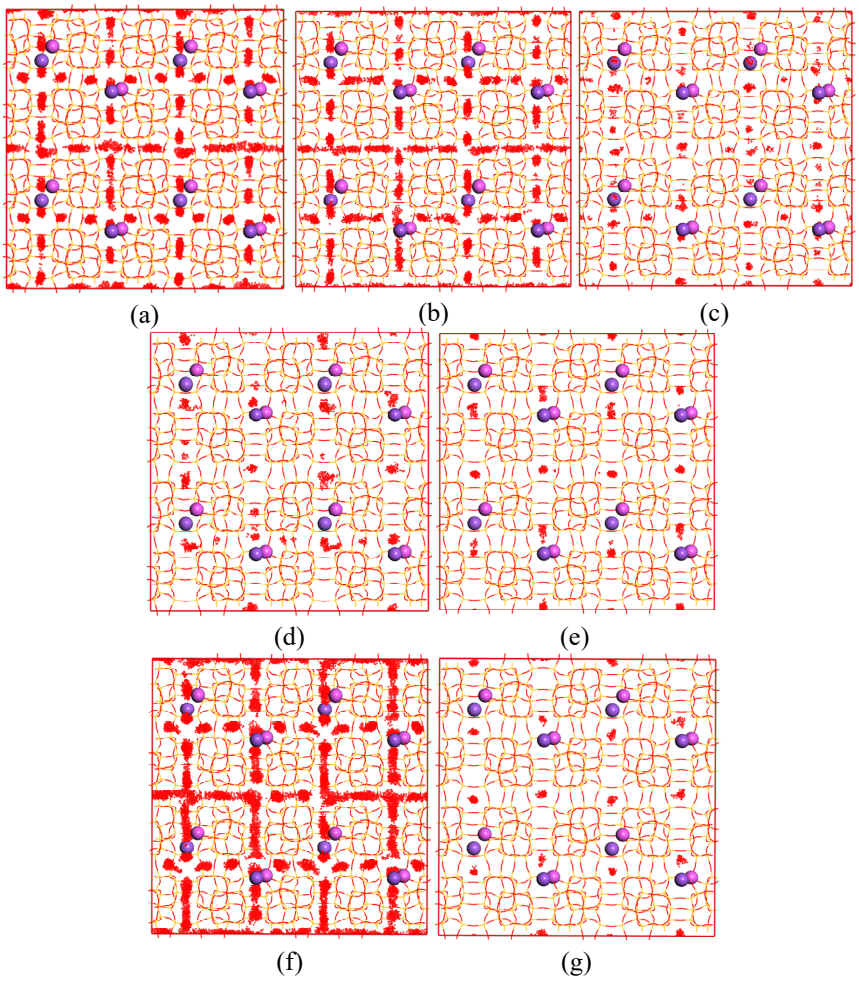

Figure 8. Distribution of possible adsorption sites in the structure of NaZSM-5 molecular sieve for five carbon-fluorine decomposition product gas molecules (**a**–**e**) and two main insulating gas molecules (**f**,**g**). (**a**) CF_3H; (**b**) CF_4; (**c**) C_2F_6; (**d**) C_3F_6; (**e**) C_3F_8; (**f**) CO_2; (**g**) C_4F_7N.

The adsorption heat is an important parameter reflecting the strength of adsorption when gas is adsorbed in the structure of the molecular sieve. The adsorption heat parameters of seven gas molecules in the molecular sieve structure were calculated. The adsorption heat probability curves of seven gas molecules in the NaZSM-5 molecular sieve structure are shown in Figure 9. The results show that the adsorption heat of the seven gas molecules in the Nazsm-5 molecular sieve is −124.0~−49.3 kJ/mol. Table 7 shows the average adsorption heat of seven gas molecules in the Nazsm-5 molecular sieve.

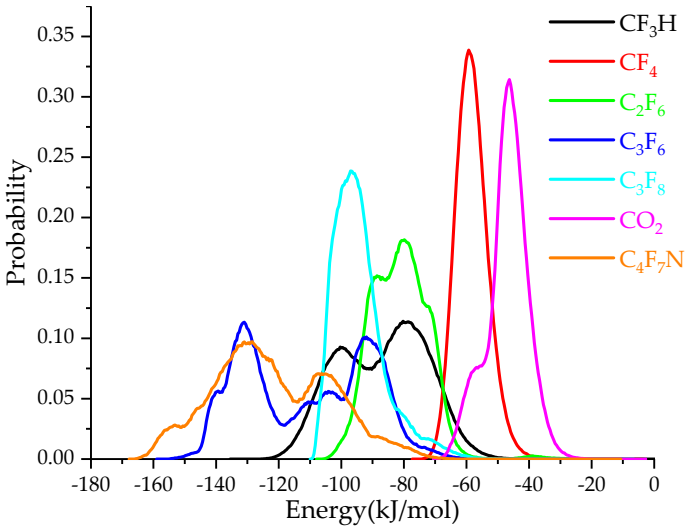

Figure 9. Probability distribution of adsorption heat of seven gas molecules on Nazsm-5 molecular sieve.

Table 7. Average adsorption heat of seven gas molecules in NaZSM-5 molecular sieve.

Type of Gas	CF_3H	CF_4	C_2F_6	C_3F_6	C_3F_8	C_4F_7N	CO_2
average adsorption heat (kJ/mol)	−89.2	−60.5	−83.5	−113.1	−96.5	−124.0	−49.3

Among the five-carbon and fluorine gas molecules, CF_4 is a non-polar molecule with a small and stable structure, and the molecular sieve structure exhibits a low heat of adsorption of −60.5 kJ/mol for it. The average adsorption heat of CF_3H is −89.2 kJ/mol and is slightly higher than that of CF_4. Although CF_3H molecule volume is smaller than CF_4, it is not easy to be bound by the molecular sieve skeleton, but its polar molecules are more likely to interact with the atoms on the skeleton to be bound, and when the molecular sieve skeleton and atomic force field act simultaneously, the two gases are subject to the same adsorption when they do molecular motion, so the adsorption rate of molecular sieve for the two gases in the adsorption experiment is approximately equal. The adsorption heat of C_2F_6 in the molecular sieve structure is between non-polar molecules (CF_4) and polar molecules (C_3F_6 and C_3F_8). Due to the symmetric structure of the C_2F_6 molecule, the molecular polarity is weak, but its larger size is more likely to interact with the atoms on the skeleton to produce strong induced attraction and then be bound in the molecular sieve skeleton, so in practice the molecular sieve material shows a certain adsorption capacity for C_2F_6. The two polar molecules C_3F_6 and C_3F_8 have larger average adsorption heats in the molecular sieve, −113.1 kJ/mol and −96.5 kJ/mol, respectively, and produce stronger interactions with the atoms in the molecular sieve. At the same time, the molecular volume of the two is large and also bound by the molecular sieve skeleton, so the NaZSM-5 molecular sieve shows a better adsorption capacity for it, and the adsorption rate of the molecular sieve for the two in the adsorption experiment is up to 80% or more.

For the two main insulating gas molecules, CO_2 and C_4F_7N, CO_2 has the smallest average adsorption heat in the molecular sieve structure at −49.3 kJ/mol, for which the NaZSM-5 molecular sieve shows a weak interaction. C_4F_7N has the largest adsorption heat in the molecular sieve structure at −124.0 kJ/mol, for which the molecular sieve is between strong physical adsorption and weak chemisorption. The NaZSM-5 molecular sieve has a strong adsorption effect on C_4F_7N. This could explain the phenomenon that the molecular sieve has a more pronounced effect on the concentration of C_4F_7N in the adsorption experiment.

The results of theoretical calculation correspond to the results of adsorption experiments. The results show that the adsorption of small non-polar gas molecules on the NaZSM-5 molecular sieve is weak, followed by small positive gas molecules. The larger chemical polarity molecules can interact with the atoms inside the molecular sieve to create an induced attraction that allows the gas to be partially absorbed. The stronger the molecular polarity, the more obvious the adsorption effect of molecular sieve structure on gas molecules, and the better the actual adsorption effect on gas.

4. Conclusions

In this paper, the adsorption properties of the ZSM-5 molecular sieve on the C_4F_7N/CO_2 mixtures and its five common fluorocarbons were investigated by gas adsorption experiments and molecular dynamics simulation. The following conclusions were obtained:

(1) ZSM-5 molecular sieve has a certain adsorption effect on six kinds of fluorocarbon gases, of which the adsorption performance of C_3F_6, and C_3F_8 is the best, with an adsorption efficiency of over 85%.

(2) The concentration of the two main insulating gases CO_2 and C_4F_7N will be affected by the ZSM-5 molecular sieve; if the insulation performance of the gas is not affected in practical application, the proportion of C_4F_7N in the mixture can be increased 1.04~1.08 times.

(3) NaZSM-5 molecular sieve has the strongest adsorption to C_4F_7N and the weakest adsorption to CO_2. The stronger the polarity of the gas molecule, the more obvious the adsorption effect of molecular sieve structure.

Author Contributions: Conceptualization, and methodology, W.L. (Wei Liu); validation, X.Q. and S.T.; resources, X.Z.; data curation, and writing—original draft preparation, Z.Y.; writing—review and editing, W.L. (Weihao Liu); supervision, and project administration, X.Z. All authors have read and agreed to the published version of the manuscript.

Funding: This research received no external funding.

Institutional Review Board Statement: Not applicable.

Informed Consent Statement: Not applicable.

Data Availability Statement: Not applicable.

Conflicts of Interest: The authors declare no conflict of interest.

References

1. Rabie, M.; Franck, C.M. Computational Screening of new High Voltage Insulation Gases with Low Global Warming Potential. *IEEE Trans. Dielectr. Electr. Insul.* **2015**, *22*, 296–302. [CrossRef]
2. Chu, F.Y. SF_6 Decomposition in Gas-Insulated Equipment. *IEEE Trans. Electr. Insul.* **1986**, *EI-21*, 693–725. [CrossRef]
3. Christophorou, L.G.; Olthoff, J.K.; Van Brunt, R.J. Sulfur hexafluoride and the electric power industry. *IEEE Electr. Insul. Mag.* **1997**, *13*, 20–24. [CrossRef]
4. Wu, Y.; Ding, D.; Wang, Y.; Zhou, C.; Lu, H.; Zhang, X. Defect recognition and condition assessment of epoxy insulators in gas insulated switchgear based on multi-information fusion. *Measurement* **2022**, *190*, 110701. [CrossRef]
5. Xiao, S.; Li, Y.; Zhang, X.; Zhuo, R.; Wang, D.; Tian, S. Discharge Decomposition Components Forming Mechanism of CF_3I Under Micro-aerobic Condition. *High Volt. Eng.* **2017**, *43*, 9.
6. Li, Y.; Zhang, X.; Fu, M.; Xiao, S.; Tang, J.; Tian, S. Research and Application Progress of Eco-Friendly Gas Insulating Medium C4F7N, Part I: Insulation and Electrical, Thermal Decomposition Properties. *Trans. China Electrotech. Soc.* **2021**, *36*, 18.

7. Gao, K.; Yan, X.; Wang, H.; He, J.; Li, Z.; Bai, C.; Liu, Y.; Huang, H. Progress in Environment-friendly Gas-insulated Transmission Line (GIL). *High Volt. Eng.* **2018**, *44*, 9.
8. Piemontesi, M.; Niemeyer, L. Sorption of SF_6 and SF_6 decomposition products by activated alumina and molecular sieve 13X. In Proceedings of the Conference Record of the IEEE International Symposium on Electrical Insulation, Montreal, QC, Canada, 16–19 June 1996.
9. Zhao, M.; Han, D.; Rong, W.; Zhang, G.; Huang, H.; Liu, Z. Decomposition Characteristics of Binary Mixtures of $(CF_3)_2CFCN$ Buffer Gases Under Corona Discharge. *High Volt. Eng.* **2019**, *45*, 76–83.
10. Kieffel, Y. Characteristics of g3—An alternative to SF6. In Proceedings of the IEEE International Conference on Dielectrics, Montpellier, France, 3 July 2017; pp. 54–57.
11. Scheels, B. Decomposition of alternative gaseous insulation under partial discharge. In Proceedings of the 20th International Symposium High Voltage Engineering, Buenos Aires, Argentina, 28 August–1 September 2017; pp. 534–539.
12. Radisavljevic, B.; Stoller, P.C.; Doiron, C.B.; Over, D.; Di-Gianni, A.; Scheel, S. Switching performance of alternative gaseous mixtures in high-voltage circuit breakers. In Proceedings of the 20th International Symposium High Voltage Engineering, Buenos Aires, Argentina, 28 August–1 September 2017; pp. 550–555.
13. Yang, T.; Zhang, B.; Li, X.; Li, C. Experimental Study of Decomposition Products of C_4F_7N/CO_2 Mixture under Different Fault Conditions. *High Volt. Eng.* **2021**, *47*, 4216–4228.
14. Su, Z.; Zhao, C. Experimental Investigation into Effects of Adsorbents on Detection of SF_6 Decomposition Products in SF_6 Equipment. *High Volt. Appar.* **2013**, *49*, 7.
15. Tang, J.; Zend, F.; Liang, X.; Qiu, Y.; Yuan, J.; Zhang, X. A Comparative Experimental Study on the Interaction of SF_6 Feature Decomposition Products with Alumina and Molecular Sieve kdhF-03. *Proc. CSEE* **2013**, *33*, 9.
16. Meyer, F.; Kieffel, Y. Application of fluoronitrile/CO_2/O_2 mixtures in high voltage products to lower the environmental footprint. In Proceedings of the Conference International des Grands Reseaux Electriques, Paris, France, 2018; pp. D1–D201.
17. Zhao, M.; Han, D.; Zhou, L.; Zhang, G. Adsorption Characteristics of Activated Alumina and Molecular Sieves for C_3F_7CN/CO_2 and Its Decomposition By-Products of Overheating Fault. *Trans. China Electrotech. Soc.* **2020**, *35*, 9.
18. Hou, H.; Yan, X.; Yu, X.; Liu, W.; Liu, Z.; Wang, B. Theoretical Investigation on the Adsorption of C_4F_7N/CO_2 Dielectric Gas and Decomposition Products in Zeolite. *High Volt. Eng.* **2019**, *45*, 8.
19. Wada, J.; Ueta, G.; Okabe, S.; Hikita, M. Dielectric Properties of Gas Mixtures with Per-Fluorocarbon Gas and Gas with Low Liquefaction Temperature. *IEEE Trans. Dielectr. Electr. Insul.* **2016**, *23*, 838–847. [CrossRef]
20. Guo, Z.; Wu, B.; Ma, X.; Chen, J. Comparative Research on the Mechanism of CO_2 and CF_3H Inhibiting Bituminous Coal Combustion. *J. Eng. Thermophys.* **2018**, *39*, 10.
21. Li, S.; Xie, S.; Wu, Y.; Liao, H. Decomposition of Greenhouse Gas of SF_6 and CF_4 by Means of Atmospheric Pressure Microwave Plasma Torch. *High Volt. Eng.* **2021**, *47*, 8.
22. Duus, H.C. Thermochemical Studies on Fluorocarbons—Heat of Formation of CF_4, C_2F_4, C_3F_6, C_2F_4 Dimer, and C_2F_4 Polymer. *Ind. Eng. Chem.* **1955**, *47*, 1445–1449. [CrossRef]
23. Wang, Y.; Ding, D.; Zhang, Y.; Yuan, Z.; Tian, S.; Zhang, X. Research on infrared spectrum characteristics and detection technology of environmental-friendly insulating medium C5F10O. *Vib. Spectrosc.* **2022**, *118*, 103336. [CrossRef]
24. Hirotani, A.; Mizukami, K.; Miura, R.; Takaba, H.; Miyamoto, A. Grand canonical Monte Carlo simulation of the adsorption of CO_2 on silicalite and NaZSM-5. *Appl. Surf. Sci.* **1997**, *120*, 81–84. [CrossRef]
25. Hu, J.; Liu, Y.; Liu, J.; Gu, C.; Wu, D. High CO_2 adsorption capacities in UiO type MOFs comprising heterocyclic ligand. *Microporous Mesoporous Mater.* **2018**, *256*, 25–31. [CrossRef]